Integrating Q Neutrosophic Soft Relation with Deep Learning based Pepper Leaf Disease Recognition for Sustainable Agriculture in KSA

Afef Selmi[1], Samah Al Zanin[2,*], Amani A. Alneil[3], Imène Issaou[4]

[1] Department of Information Technology, College of Computer, Qassim University, Buraydah, Saudi Arabia.
[2] Department of Computer Science, College of Computer Engineering and Sciences, Prince Sattam bin Abdulaziz University, Kharj, Saudi Arabia.
[3] Department of Computer and Self Development, Preparatory Year Deanship, Prince Sattam bin Abdulaziz University, AlKharj, Saudi Arabia.
[4] Unit of Scientific Research, Applied College, Qassim University, Buraydah, Saudi Arabia.
Emails: a.selmi@qu.edu.sa; s.alzanin@psau.edu.sa; aa.mohammad@psau.edu.sa; I.ISSAOUI@qu.edu.sa

Abstract

Sustainable agriculture is of utmost importance in Saudi Arabia to resolve problems like environmental degradation and water scarcity. The country has made considerable investments in modern agricultural systems such as vertical farming and hydroponics to maximize crop yields and water efficiency. The most direct manifestation of earlier crop growth problems is Pepper leaf disease. Rapid and accurate detection of pepper leaf disease is crucial to immediately detect growth issues and enable accurate control and preventive measures. The traditional method based on human experience and visual inspection to recognize pepper leaves is costly, subjective and laborious. Hence, it is essential to develop fast, convenient, and precise techniques for identifying pepper leaf disease. The Q-neutrosophic soft relation is a generalization that integrates the concepts of soft set and neutrosophic set, enabling for truth, indeterminacy, and false degree in the membership of element with respect to a relation in a soft computing framework. Therefore, this study introduces a new Q Neutrosophic Soft Relation with Deep Learning based Pepper Leaf Disease Recognition (QNSRDL-PLDR) technique for Sustainable Agriculture in KSA. The proposed QNSRDL-PLDR method leverages DenseNet for feature extraction, the model uses the Adam optimizer for effective parameter optimization. Unique to this framework is the combination of a Q-neutrosophic soft relation classifier, allowing nuanced classification considering truth, indeterminacy, and falsity degrees in disease presence assessment. A comprehensive set of simulations is conducted to demonstrate the better efficiency of the QNSRDL-PLDR technique. This technique aims to improve reliability and accuracy in detecting Pepper Leaf Diseases, critical for crop management and sustainable agricultural practices

Keywords: Leaf Disease Recognition; Deep Learning; Neutrosophic Soft; Sustainable Agriculture; DenseNet

1. Introduction

Presently, numerous uncertainty issues come across in various areas of everyday life, like engineering and physics [1]. While neutrosophic soft set is very effective in stating neutral uncertain data, this mathematical technique is unsatisfactory if the size of uncertain data upsurges [2]. To overcome these challenges, Q-neutrosophic soft set, are developed for handling 2D uncertain data [3]. Generally, pepper is nearly a vital crop and is directly linked to the rate of human obesity and cardiovascular illness. The need for peppers increases every day with the fast development of global populace [4]. Diseases like pepper anthracnose, pepper white spot illness and pepper powdery mildew are the major causes affecting the harvest and excellence of pepper. Pepper leaf illnesses are normally the straightest appearance of initial crop growth issues [5]. Fast and precise detection of pepper leaf illnesses is vital for quickly detecting evolution problems and allowing precise control and prevention methods [6]. The traditional methods are commonly based on visual assessment and knowledge of humans for identifying

DOI: https://doi.org/10.54216/IJNS.250117
Received: April 27, 2024 Revised: June 05, 2024 Accepted: June 29, 2024

pepper leaves is biased, time-consuming and expensive. So, it is necessary to grow an accurate, quick, and appropriate model to detect pepper leaf illnesses [7].

The use of automatic techniques to identify plant illnesses is very important in defending crops. Spectral reflection of unhealthy and healthy plants varies in the detectable and near-infrared area [8]. Therefore, spectral reflections are employed to identify plant diseases. Dissimilar classification techniques like Principle Component Analysis (PCA), Nearest Neighbor, Artificial Neural Network (ANN), Probabilistic Neural Networks (PNN), Support Vector Machines (SVM), and Fuzzy Logic are employed with spectral reflections of plants. Due to the improvement of artificial intelligence (AI) model, deep learning (DL) was projected to resolve composite vision tasks [9]. In the area of farming, dissimilar DL models were explored for the detection of the symptoms of main illnesses that affect harvests. Particularly Convolutional Neural Networks (CNNs) are the most useful method, which was successfully employed in crop leaf illness detection [10].

This study introduces a new Q-Neutrosophic Soft Relation with Deep Learning based Pepper Leaf Disease Recognition (QNSRDL-PLDR) technique for Sustainable Agriculture in KSA. The proposed QNSRDL-PLDR method leverages DenseNet for feature extraction, the model uses the Adam optimizer for effective parameter optimization. Unique to this framework is the combination of a Q-neutrosophic soft relation classifier, allowing nuanced classification considering truth, indeterminacy, and falsity degrees in disease presence assessment. A comprehensive set of simulations is conducted to demonstrate the better performance of the QNSRDL-PLDR method.

2. Related Works

Priya and Vijayarani [11] developed a detection and classification method (DCM) utilizing deep CNN (DCNN) method. In the first step, augmentation models are employed in order to upsurge the size of dataset, to decrease noise, and to eliminate annoying background noise from imageries of leaves. Additionally, augmented imageries are set to the CNN with many layers of pooling and convolution layers, which are employed for identifying and classifying unhealthy plants. Perveen et al. [12] presented a multiscale U-system for effectual parallel analysis and classification of tomato leaf lesions. This technique uses multi-scale residual units. The Classifier and Bridge (CB) unit is presented. In the phase of segmentation, the activation mapping of an exact type is deconvoluted utilizing a mixture of convolution and up-sampling. A dual cross-entropy loss function, and restricted amount of pixel-level labels are used. Chen et al. [13] presented a method, which unites channel attention and channel pruning named CACPNET, appropriate for illness classification of general class. The device of channel attention implements a local cross-channel tactic without dimensional decrease that was implanted into a ResNet18-based method, which unites the average pooling with max-pooling to efficiently enhance the feature-removing capability of plant leaf illnesses. Depending upon the optimal feature extractor state, insignificant networks were extracted to decrease the parameters of method and density through the local ratio of compression and L1 norm channel weight.

Sarawagi et al. [14] proposed a new CNN design. The technique gathers disease-specific features from input images by utilizing data augmentation models to preciously increase the training dataset. ReLU-activated convolutional layers slowly seizure features at dissimilar levels, from lower to higher, while max pooling layers reduce spatial dimensionality. Once the features are removed, full connection (FC) layers with an activation function of softmax categorize them into disease sets. Abisha et al. [15] presented an advanced technique to identify and classify diseased brinjal leaves utilizing DCNN and Radial Basis FFNN (RBFNN). In the initial stage, the novel plant leaf was pre-processed by a Gaussian filter (GF). Then, a segmentation model depending upon expectation and maximization (EM) was exploited to part the leaf unhealthy areas. Afterwards, the discrete Shearlet transform (DTS) was employed in order to remove the foremost feature of imageries, which are then combined in order to yield vectors. Finally, DCNN and RBFNN are employed for identification.

In [16], a novel pepper disease detection method based on the TPSAO-AMWNet has been projected. In initial step, an Adaptive Residual Pyramid Convolution (ARPC) framework united with the Squeeze-and-Excitation (SE) unit was developed by using channel attention and adaptively; next, to find out the problem of micro-feature extractor, Minor Triplet Disease Focus Attention (MTDFA) has been developed; next, a diverse loss function uniting Weighted Focal Loss and L2 regularization (WfrLoss) was presented. Then, the tent particle snow ablation optimizer (TPSAO) is planned for precisely identifying the most effective rate of learning. Rababa et al. [17] presented a DL structure, which is specially intended to mechanically identify Pepper leaf imageries as both healthy and diseased with germs. In particular, the DeepNet method has been perfected utilizing domain-specific Pepper leaf imageries. Moreover, PCA model is employed in the DeepNet input image to remove and pick the most distinguishing feature.

DOI: https://doi.org/10.54216/IJNS.250117
Received: April 27, 2024 Revised: June 05, 2024 Accepted: June 29, 2024

3. Proposed Methodology

In this study, we have developed a new QNSRDL-PLDR method for sustainable agriculture in KSA. The main purposes of the QNSRDL-PLDR technique include three distinct processes feature extraction, parameter optimizer, and classification process. Fig. 1 represents the workflow of QNSRDL-PLDR technique.

A. Feature Extraction

DenseNets introduce the initial departure from ResNets in how information is transmitted [18]. DenseNets concatenates mapping features of resultant layer with incoming mapping features rather than adding them. Therefore, this calculation shows that Eq. (1)

$$x_l = H_l([x_0 + x_1 + .. + x_{l-1}]) \quad (1)$$

We encountered a related challenge in our research on ResNets, the integrating performance of mapping features can be difficult once they are of distinct sizes even though the integrating action is a calculation or concatenation of mapping features. Thus, in the same manner it can be utilized for ResNets, DenseNets can be separated as dense blocks. In a partnership, the size of mapping features endure the similar, then the count of filters variations among them. These layers among the dense blocks are named Transition Layer. It can be utilized for down-sampling by executing batch normalization (BN), 1x1 convolutional, and 2x2 pooling layers. Due to the concatenation of mapping features, the channel size is enhanced at every layer. 'k' defines the rate of growth parameter that preserves the data counts kept in all the network layers. If H_1 makes k mapping features after the generalization formula to define the mapping feature counts by l^{th} layer is as expressed in Eq. (1).

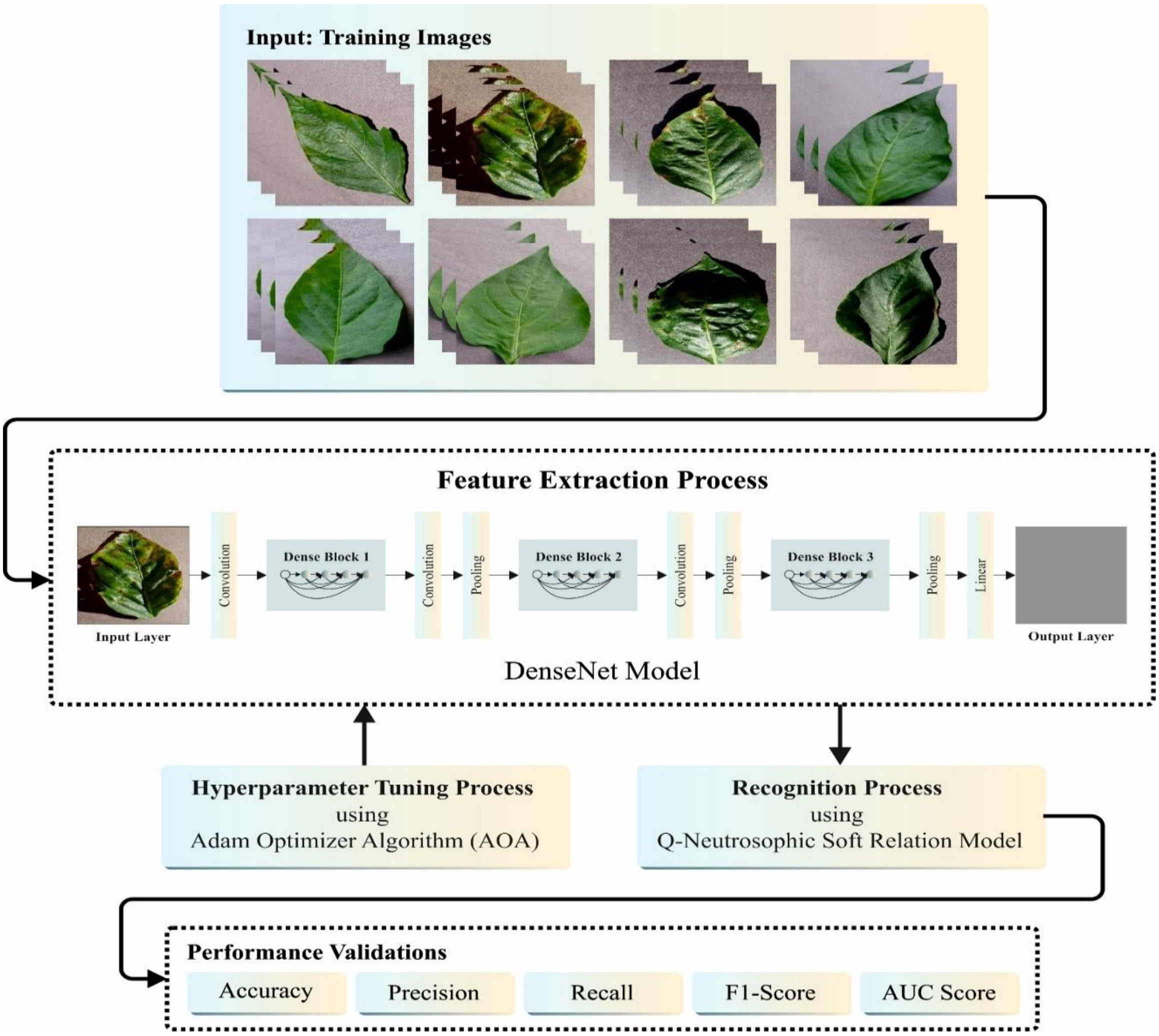

Figure 1: Workflow of QNSRDL-PLDR technique

DOI: https://doi.org/10.54216/IJNS.250117
Received: April 27, 2024 Revised: June 05, 2024 Accepted: June 29, 2024

Mapping features perform learning data. Each layer takes access to mapping features of prior layers, and so it takes combined knowledge. All the layers enhance original data or mapping features to this combined data, in concrete k mapping features of data. Accordingly, DenseNet uses and stores the data from prior layers superior to ResNets and standard ConvNet.

B. Parameter Optimizer

The Adam algorithm is an optimization technique to update parameters within NNs, well-known for its adaptive learning algorithm [19]. It dynamically adjusts the learning rate according to the gradient variation of parameters, considerably improving the generalizability and the efficiency of training model. Adam achieves better convergence rates by combining the strength of the RMSProp and momentum gradient descent algorithm.

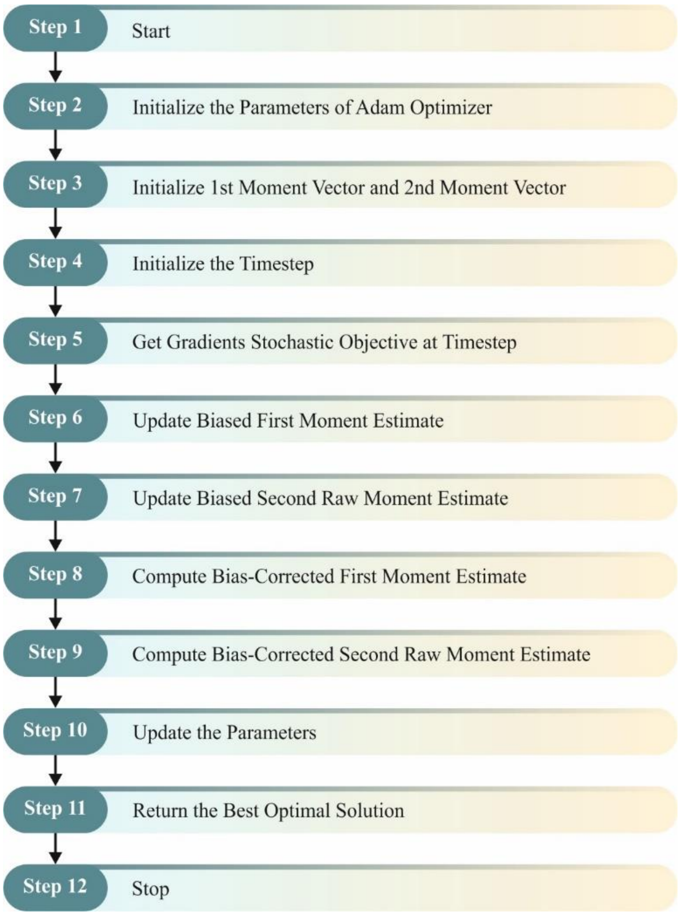

Figure 2: Steps involved in Adam optimizer

Adam exploits 1st and 2nd order moment estimates in the parameter updating procedure, which facilitates an accelerated gradient descent algorithm. This enables Adam to quickly converge towards optimum solution fine-tune the speed and update trajectory model parameters with high accuracy.

$$v(t) = \mu v(t-1) + (1-\mu) g(t) \tag{2}$$

Where $v(t)$ is the moment of t times, μ is a hyperparameter, and $g(t)$ is the gradient value.

$$m(t) = \beta 1 m(t-1) + (1-\beta 1) g(t) \tag{3}$$

$$s(t) = \beta 2 s(t-1) + (1-\beta 2) g^2(t) \tag{4}$$

$$\alpha(t) = \frac{\eta \mu^t}{\sqrt{s(t)} + \varepsilon} \tag{5}$$

DOI: https://doi.org/10.54216/IJNS.250117
Received: April 27, 2024 Revised: June 05, 2024 Accepted: June 29, 2024

Here $\beta 1$ and $\beta 2$ are control gradient hyperparameters; $m(t)$and $s(t)$, are average and square gradient moving averages, $\alpha(t)$ are the mean and adaptive learning rate values, correspondingly; $g(t)$ refers to the gradient values; and ε denotes the offset term.

The model's capability to modulate the learning rate across parameter gradient contributed to model generalization and better effectiveness. Furthermore, the integration of 1st and 2nd order moments allows Adam to deal with the velocity and directionality of parameter updates, which foster better convergence. The steps involved in Adam optimizer is depicted in Fig. 2.

The Adam optimizer is used to derive an FF for attaining superior classifier outcomes. It defines a positive integer to describe the enhanced outcomes of the solute on candidate. Here, the decline of the classifier error rate is regarded as an FF.

$$fitness(x_i) = ClassifierErrorRate(x_i)$$
$$= \frac{No.of\ misclassified\ samples}{Total\ No.of\ samples} * 100 \quad (6)$$

C. Recognition Process

The idea of Cartesian product (CP) is defined for the two Q-NS sets considering the adapted Q-NS-set, and hence we describe the concept of Q-NS-set [20]. Next, the inverse and composition operations are given for the relationship with some fundamental characteristics.

Consider $(\hat{\Gamma}_Q, P)$, $(\hat{\Lambda}_Q, P) \in 2^{NS_Q(U)}$. Next, $(\hat{\Gamma}_Q, P) \times (\hat{\Lambda}_Q, P) = (\hat{\Omega}_Q, P \times P)$ represents the CP of $(\hat{\Gamma}_Q, P)$ and $(\hat{\Lambda}_Q, P)$, whereas $(a, b) \in P \times P$, $\hat{\Omega}_Q: P \times P \to 2^{NS_Q(U)}$ and $\hat{\Omega}_Q(a, b) = \Gamma(a)_Q \times \Lambda(b)_Q$, viz.,

$$\left(\hat{\Omega}_Q, P \times P\right) = \left\{\left((a, b), \hat{\Omega}_Q(a, b)\right) : (a, b) \in P \times P\right\} \quad (7)$$

Thus

$$\hat{\Omega}_Q(a, b) = \left\{\langle (u, q), T_{\hat{\Omega}_Q(a,b)}(u, q), I_{\hat{\Omega}_Q(a,b)}(u, q), F_{\hat{\Omega}_Q(a,b)}(u, q)\rangle : (u, q) \in U \times Q\right\} \quad (8)$$

Where $T_{\hat{\Omega}_Q(a,b)}(u, q), I_{\hat{\Omega}_Q(a,b)}(u, q), F_{\hat{\Omega}_Q(a,b)}(u, q)$ denotes the truth, indeterminacy and false degree of $(\hat{\Omega}_Q, P \times P)$ thus $T_{\hat{\Omega}_Q(a,b)}, I_{\hat{\Omega}_Q(a,b)}, F_{\hat{\Omega}_Q(a,b)}(u){:}U \to [0, 1]$ and for $(u, q) \in U \times Q$ and $(a, b) \in P \times P$ such that:

$$T_{\hat{\Omega}_Q(a,b)}(u, q) = \min\left\{T_{\hat{\Gamma}_Q(a)}(u, q), T_{\hat{\Lambda}_Q(b)}(u, q)\right\},$$

$$I_{\hat{\Omega}_Q(a,b)}(u, q) = \max\{I_{\hat{\Gamma}_Q(a)}(u, q), I_{\hat{\Lambda}_Q(b)}(u, q)\}$$

and

$$F_{\hat{\Omega}_Q(a,b)}(u, q) = \max\left\{F_{\hat{\Gamma}_Q(a)}(u, q), F_{\hat{\Lambda}_Q(b)}(u, q)\right\}.$$

Consider $U = \{u_1, u_2, u_3\}$, $Q = \{q_1, q_2\}$, $P = \{p_1, p_2\}$, $(\hat{\Gamma}_Q, P)$ and Q-NS-set $(\hat{\Lambda}_Q, P)$ over U is represented by:

$$(\hat{\Lambda}_Q, P) = \left\{\begin{array}{c}\left(\begin{array}{c}\langle (u_1, q_1), 0.76, 0.56, 0.85\rangle, \langle (u_1, q_2), 0.84, 0.65, 0.24\rangle,\\ p_1, \langle (u_2, q_1), 0.18, 0.56, 0.43\rangle, \langle (u_2, q_2), 0.72, 0.56, 0.62\rangle,\\ \langle (u_3, q_1), 0.45, 0.24, 0.37\rangle, \langle (u_3, q_2), 0.32, 0.54, 0.41\rangle\end{array}\right),\\ \left(\begin{array}{c}\langle (u_1, q_1), 0.36, 0.52, 0.44\rangle, \langle (u_1, q_2), 0.82, 0.54, 0.78\rangle,\\ p_2, \langle (u_2, q_1), 0.28, 0.68, 0.55\rangle, \langle (u_2, q_2), 0.66, 0.48, 0.59\rangle,\\ \langle (u_3, q_1), 0.25, 0.56, 0.74\rangle, \langle (u_3, q_2), 0.92, 0.64, 0.25\rangle\end{array}\right)\end{array}\right\}.$$

Next, $(\hat{\Omega}_Q, P \times P) = (\hat{\Gamma}_Q, P) \times (\hat{\Lambda}_Q, P)$ is

$(\hat{\Omega}_Q, P \times P) = \{\hat{\Gamma}_Q(p_1) \times \hat{\Lambda}_Q(p_1), \hat{\Gamma}_Q(p_1) \times \hat{\Lambda}_Q(p_2), \hat{\Gamma}_Q(p_2) \times \hat{\Lambda}_Q(p_1), \hat{\Gamma}_Q(p_2) \times \hat{\Lambda}_Q(p_2)\}$

Where

DOI: https://doi.org/10.54216/IJNS.250117
Received: April 27, 2024 Revised: June 05, 2024 Accepted: June 29, 2024

$$\hat{\Gamma}_Q(p_1) \times \hat{\Lambda}_Q(p_1) = \begin{Bmatrix} \langle (u_1, q_1), 0.55,0.76,0.85\rangle, \langle (u_1, q_2), 0.47,0.65,0.72\rangle, \\ \langle (u_2, q_1), 0.18,0.56,0.43\rangle, \langle (u_2, q_2), 0.72,0.56,0.67\rangle, \\ \langle (u_3, q_1), 0.45,0.62,0.45\rangle, \langle (u_3, q_2), 0.32,0.74,0.47\rangle \end{Bmatrix}$$

Consider $(\hat{\Gamma}_Q, P)$, $(\hat{\Lambda}_Q, P) \in 2^{NSQ(U)}$. Next, a Q-NS-set from $(\hat{\Gamma}_Q, P)$ to $(\hat{\Lambda}_Q, P)$ is a Q-NS-subclass of $(\hat{\Gamma}_Q, P) \times (\hat{\Lambda}_Q, P)$, and $(\hat{\mathfrak{R}}_Q, K \times L)$, where $K \times L \subseteq P \times P$ and $\hat{\mathfrak{R}}_Q(a, b) \subseteq (\hat{\Gamma}_Q, P) \times (\hat{\Lambda}_Q, P)$, $\forall (a, b) \in K \times L$, viz.,

$$(\hat{\mathfrak{R}}_Q, K \times L) = \left\{\left((a, b), \hat{\mathfrak{R}}_Q(a, b)\right) : (a, b) \in K \times L \subseteq P \times P\right\} \quad (9)$$

Thus

$$\hat{\mathfrak{R}}_Q(a, b) = \left\{\langle (u, q), T_{\hat{\mathfrak{R}}_Q(a,b)}(u, q), I_{\hat{\mathfrak{R}}_Q(a,b)}(u, q), F_{\hat{\mathfrak{R}}_Q(a,b)}(u, q)\rangle : (u, q) \in U \times Q\right\} \quad (10)$$

Where

$$T_{\hat{\mathfrak{R}}_Q(a,b)}(u, q) = \min\left\{T_{\hat{\Gamma}_Q(a)}(u, q), T_{\hat{\Lambda}_Q(b)}(u, q)\right\},$$

$$I_{\hat{\mathfrak{R}}_Q(a,b)}(u, q) = \max\left\{I_{\hat{\Gamma}_Q(a)}(u, q), I_{\hat{\Lambda}_Q(b)}(u, q)\right\}$$

and

$$F_{\hat{\mathfrak{R}}_Q(a,b)}(u, q) = \max\left\{F_{\hat{\Gamma}_Q(a)}(u, q), F_{\hat{\Lambda}_Q(b)}(u, q)\right\}.$$

If $(\hat{\mathfrak{R}}_Q, K \times L)$ is a Q-NS-set from $(\hat{\Gamma}_Q, P)$ to $(\hat{\Gamma}_Q, P)$, then is known as a Q-NS-set on $(\hat{\Gamma}_Q, P)$.

Assume $\hat{\mathfrak{R}}_Q$ as a Q-NS-set on $(\hat{\Gamma}_Q, P)$. Then,

(i) The range of $\hat{\mathfrak{R}}_Q(\widehat{DM}_{\hat{\mathfrak{R}}_Q})$ can be described as a Q-NS-set $(\widehat{DM}_{\hat{\mathfrak{R}}_Q}, K_1)$, where $K_1 = \{a \in K : \hat{\mathfrak{R}}_Q(a, b) \in \hat{\mathfrak{R}}_Q, \exists b \in L\}$ and $\widehat{DM}_{\hat{\mathfrak{R}}_Q}(a_1) = \hat{\Gamma}_Q(a_1), \forall a_1 \in K_1$.

(ii) The domain of $\hat{\mathfrak{R}}_Q(\widehat{RN}_{\hat{\mathfrak{R}}_Q})$ can be described as a Q-NS-set $(\widehat{RN}_{\hat{\mathfrak{R}}_Q}, L_1)$ where $L_1 = \{b \in L : \hat{\mathfrak{R}}_Q(a, b) \in \hat{\mathfrak{R}}_Q, \exists a \in K\}$ and $\widehat{RN}_{\hat{\mathfrak{R}}_Q}(b_1) = \hat{\Lambda}_Q(b_1), \forall b_1 \in L_1$.

Consider $\hat{\mathfrak{R}}_Q = \{\hat{\Gamma}_Q(p_1) \times \hat{\Lambda}_Q(p_1), \hat{\Gamma}_Q(p_1) \times \hat{\Lambda}_Q(p_2)\} \subseteq (\hat{\Gamma}, P) \times (\hat{\Lambda}, P)$ as a Q-NS-set. Next, $\widehat{DM}_{\hat{\mathfrak{R}}_Q} = (\widehat{DM}_{\hat{\mathfrak{R}}_Q}, K_1)$ where $\widehat{DM}_{\hat{\mathfrak{R}}_Q}(p_1) = \hat{\Gamma}_Q(p_1)$ for $K_1 = \{p_1\}$ and $\widehat{RN}_{\hat{\mathfrak{R}}} = (\widehat{RN}, L_1)$ where $\widehat{RN}_{\hat{\mathfrak{R}}}(p_1) = \hat{\Lambda}_Q(p_1), \widehat{RN}_{\hat{\mathfrak{R}}}(p_2) = \hat{\Lambda}_Q(p_2)$ for $L_1 = \{p_1, p_2\}$.

The identity Q-NS-set $\hat{I}_{(\hat{\Gamma}_Q, P)}$ on a Q-NS-set $(\hat{\Gamma}_Q, P)$ is represented by $\hat{\Gamma}_Q(a)\hat{I}_{(\hat{\Gamma}_Q, P)}\hat{\Gamma}_Q(b)$ if and only if $a = b$, then

$$(\hat{\mathfrak{R}}_Q, K \times L) = \left\{\begin{pmatrix} & \langle (u_1, q_1), 0.55, 0.76, 0.85\rangle, \langle (u_1, q_2), 0.47, 0.65, 0.72\rangle, \\ (p_1, p_1), & \langle (u_2, q_1), 0.18, 0.56, 0.43\rangle, \langle (u_2, q_2), 0.72, 0.56, 0.67\rangle, \\ & \langle (u_3, q_1), 0.45, 0.62, 0.45\rangle, \langle (u_3, q_2), 0.32, 0.74, 0.47\rangle \end{pmatrix}, \begin{pmatrix} & \langle (u_1, q_1), 0.36, 0.52, 0.44\rangle, \langle (u_1, q_2), 0.48, 0.65, 0.78\rangle, \\ (p_2, p_2), & \langle (u_2, q_1), 0.23, 0.68, 0.75\rangle, \langle (u_2, q_2), 0.35, 0.74, 0.85\rangle, \\ & \langle (u_3, q_1), 0.25, 0.56, 0.74\rangle, \langle (u_3, q_2), 0.89, 0.64, 0.32\rangle \end{pmatrix}\right\}$$

is an identity Q-NS-set.

Consider $(\hat{\Gamma}_Q, P)$, $(\hat{\Lambda}_Q, P) \in 2^{NSQ(U)}$ and $(\hat{\mathfrak{R}}_Q, K \times L)$ as a Q-NS-set from $(\hat{\Gamma}, P)$ to $(\hat{\Lambda}, P)$. Next, the inverse of $(\hat{\mathfrak{R}}_Q, K \times L)$, $(\hat{\mathfrak{R}}_Q^{-1}, L \times K)$ is a Q-NS-set and is represented by:

$$\hat{\mathfrak{R}}_Q^{-1}(b, a) = \hat{\mathfrak{R}}_Q(a, b), \forall (a, b) \in K \times L \subseteq P \times P.$$

$\hat{\mathfrak{R}}_Q^{-1} = \{\hat{\Lambda}_Q(p_1) \times \hat{\Gamma}_Q(p_1), \hat{\Lambda}_Q(p_2) \times \hat{\Gamma}_Q(p_1)\} \subseteq (\hat{\Lambda}, P) \times (\hat{\Gamma}, P)$.

Assume $(\hat{\Gamma}_Q, P)$, $(\hat{\Lambda}_Q, P) \in 2^{NSQ(U)}$ and $(\hat{\mathfrak{R}}_Q^1, K \times L)$, $(\hat{\mathfrak{R}}_Q^2, K \times L)$ are Q-NS- set from $(\hat{\Gamma}_Q, P)$ to $(\hat{\Lambda}_Q, P$

DOI: https://doi.org/10.54216/IJNS.250117
Received: April 27, 2024 Revised: June 05, 2024 Accepted: June 29, 2024

(i) $((\widehat{\Re}_Q^1, K \times L)^{-1})^{-1} = (\widehat{\Re}_Q^1, K \times L)$.

(ii) $(\widehat{\Re}_Q^1, K \times L) \widehat{\subseteq} (\widehat{\Re}_Q^2, K \times L) \Rightarrow (\widehat{\Re}_Q^1, K \times L)^{-1} \widehat{\subseteq} (\widehat{\Re}_Q^2, K \times L)^{-1}$

Since $((\widehat{\Re}_Q^1)^{-1})^{-1} = \widehat{\Re}_Q^1(a,b)$, then $((\widehat{\Re}_Q^1, K \times L)^{-1})^{-1} = (\widehat{\Re}_Q^1, K \times L); \forall (a,b) \in K \times L \subseteq P \times P$.

(ii) $\widehat{\Re}_Q^1(a,b) \subseteq \widehat{\Re}_Q^2(a,b) \Rightarrow (\widehat{\Re}_Q^1)^{-1}(b,a) \subseteq (\widehat{\Re}_Q^2)^{-1}(b,a)$ and we have

$$(\widehat{\Re}_Q^1, K \times L)^{-1} \widehat{\subseteq} (\widehat{\Re}_Q^2, K \times L)^{-1}; \forall (a,b) \in K \times L \subseteq P \times P.$$

Consider $(\hat{\Gamma}_Q, P)$, $(\hat{\Lambda}_Q, P)$, $(\hat{\Omega}_Q, P) \in 2^{NS_Q(U)}$ and $(\widehat{\Re}_Q^1, K \times L)$, $(\widehat{\Re}_Q^2, L \times M)$ as Q-NS-set from $(\hat{\Gamma}_Q, P)$ to $(\hat{\Lambda}_Q, P)$ and from $(\hat{\Lambda}_Q, P)$ to $(\hat{\Omega}_Q, P)$ correspondingly, where $(a,b) \in K \times L \subseteq P \times P$ and $(b,c) \in L \times M \subseteq P \times P$, then the composition of Q-NS-sets $(\widehat{\Re}_Q^1, K \times L)$ and $(\widehat{\Re}_Q^2, L \times M)$ represented as $\widehat{\Re}_Q^2 \circ \widehat{\Re}_Q^1$ from $(\hat{\Gamma}_Q, P)$ to $(\hat{\Omega}_Q, P)$ is given below:

$$\left(\widehat{\Re}_Q^2 \circ \widehat{\Re}_Q^1, K \times M\right) = \left\{\left((a,c), \left(\widehat{\Re}_Q^2 \circ \widehat{\Re}_Q^1\right)(a,c)\right) : (a,c) \in K \times M \subseteq P \times P\right\} \quad (11)$$

Thus

$$\left(\widehat{\Re}_Q^2 \circ \widehat{\Re}_Q^1\right)(a,c) = \left\{ \begin{matrix} T_{(\widehat{\Re}_Q^2 \circ \widehat{\Re}_Q^1)(a,c)}(u,q), \\ \langle (u,q), T_{(\widehat{\Re}_Q^2 \circ \widehat{\Re}_Q^1)(a,c)}(u,q) \rangle : (u,q) \in U \times Q \\ F_{(\widehat{\Re}_Q^2 \circ \widehat{\Re}_Q^1)(a,c)}(u,q) \end{matrix} \right\} \quad (12)$$

Where

$$T_{(\widehat{\Re}_Q^2 \circ \widehat{\Re}_Q^1)(a,c)}(u,q) = \max\{T_{\widehat{\Re}_Q^1(a,b)}(u,q), T_{\widehat{\Re}_Q^2(b,c)}(u,q)\}$$

$$= \max\{\min\{T_{\hat{\Gamma}_Q(a)}(u,q), T_{\hat{\Lambda}_Q(b)}(u,q)\}, \min\{T_{\hat{\Lambda}_Q(b)}(u,q), T_{\hat{\Omega}_Q(c)}(u,q)\}\},$$

$$I_{(\widehat{\Re}_Q^2 \circ \widehat{\Re}_Q^1)(a,c)}(u,q) = \min\{I_{\widehat{\Re}_Q^1(a,b)}(u,q), I_{\widehat{\Re}_Q^2(b,c)}(u,q)\}$$

$$= \min\{\max\{I_{\hat{\Gamma}_Q(a)}(u,q), I_{\hat{\Lambda}_Q(b)}(u,q)\}, \max\{I_{\hat{\Lambda}_Q(b)}(u,q), I_{\hat{\Omega}_Q(c)}(u,q)\}\},$$

$$F_{(\widehat{\Re}_Q^2 \circ \widehat{\Re}_Q^1)(a,c)}(u,q) = \min\{F_{\widehat{\Re}_Q^1(a,b)}(u,q), F_{\widehat{\Re}_Q^2(b,c)}(u,q)\}$$

$$= \min\{\max\{F_{\hat{\Gamma}_Q(a)}(u,q), F_{\hat{\Lambda}_Q(b)}(u,q)\},$$

$$\max\{F_{\hat{\Lambda}_Q(b)}(u,q), F_{\hat{\Omega}_Q(c)}(u,q)\}\}.$$

Consider $U = \{u_1, u_2\}$ as a set of televisions, $Q = \{q_1$: philips, q_2: sony$\}$ as a set of brands, $P = \{p_1, p_2, p_3\}$ as the set of parameters that should be inspected for the various brands of television. For $i = 1,2,3,4$, the parameter p_i represents "fun to watch", "expensive", "modern" and "easy to use", correspondingly.

Assume television views as Q-NS-set $(\hat{\Gamma}_Q, P)$, $(\hat{\Lambda}_Q, P)$ and $(\hat{\Omega}_Q, P)$ as follows:

$$(\hat{\Gamma}_Q, P) = \left\{ \begin{matrix} \left(p_1, \begin{matrix} \langle (u_1,q_1), 0.23, 0.44, 0.36 \rangle, \langle (u_1,q_2), 0.44, 0.55, 0.75 \rangle, \\ \langle (u_2,q_1), 0.25, 0.47, 0.38 \rangle, \langle (u_2,q_2), 0.77, 0.52, 0.84 \rangle \end{matrix}\right), \\ \left(p_2, \begin{matrix} \langle (u_1,q_1), 0.15, 0.64, 0.53 \rangle, \langle (u_1,q_2), 0.48, 0.62, 0.88 \rangle, \\ \langle (u_2,q_1), 0.74, 0.34, 0.25 \rangle, \langle (u_2,q_2), 0.12, 0.46, 0.77 \rangle \end{matrix}\right), \\ \left(p_3, \begin{matrix} \langle (u_1,q_1), 0.65, 0.84, 0.14 \rangle, \langle (u_1,q_2), 0.35, 0.57, 0.79 \rangle, \\ \langle (u_2,q_1), 0.49, 0.57, 0.89 \rangle, \langle (u_2,q_2), 0.91, 0.26, 0.72 \rangle \end{matrix}\right), \\ \left(p_4, \begin{matrix} \langle (u_1,q_1), 0.53, 0.3, 0.25 \rangle, \langle (u_1,q_2), 0.77, 0.87, 0.93 \rangle, \\ \langle (u_2,q_1), 0.22, 0.32, 0.19 \rangle, \langle (u_2,q_2), 0.39, 0.86, 0.24 \rangle \end{matrix}\right) \end{matrix} \right\},$$

DOI: https://doi.org/10.54216/IJNS.250117
Received: April 27, 2024 Revised: June 05, 2024 Accepted: June 29, 2024

$$(\hat{\Lambda}_Q, P) = \left\{ \begin{array}{l} \left(p_1, \begin{array}{c} \langle (u_1,q_1), 0.53,0.31,0.91\rangle, \langle (u_1,q_2), 0.16,0.72,0.83\rangle, \\ \langle (u_2,q_1), 0.73,0.88,0.15\rangle, \langle (u_2,q_2), 0.61,0.24,0.43\rangle \end{array}\right), \\ \left(p_2, \begin{array}{c} \langle (u_1,q_1), 0.33,0.54,0.74\rangle, \langle (u_1,q_2), 0.56,0.79,0.98\rangle, \\ \langle (u_2,q_1), 0.42,0.18,0.55\rangle, \langle (u_2,q_2), 0.67,0.44,0.77\rangle \end{array}\right), \\ \left(p_3, \begin{array}{c} \langle (u_1,q_1), 0.65,0.84,0.14\rangle, \langle (u_1,q_2), 0.35,0.57,0.79\rangle, \\ \langle (u_2,q_1), 0.49,0.57,0.89\rangle, \langle (u_2,q_2), 0.91,0.26,0.72\rangle \end{array}\right), \\ \left(p_4, \begin{array}{c} \langle (u_1,q_1), 0.53,0.3,0.25\rangle, \langle (u_1,q_2), 0.77,0.87,0.93\rangle, \\ \langle (u_2,q_1), 0.22,0.32,0.19\rangle, \langle (u_2,q_2), 0.39,0.86,0.24\rangle \end{array}\right) \end{array} \right\},$$

$$(\hat{\Omega}_Q, P) = \left\{ \begin{array}{l} \left(p_1, \begin{array}{c} \langle (u_1,q_1), 0.23,0.44,0.36\rangle, \langle (u_1,q_2), 0.44,0.55,0.75\rangle, \\ \langle (u_2,q_1), 0.25,0.47,0.38\rangle, \langle (u_2,q_2), 0.77,0.52,0.84\rangle \end{array}\right), \\ \left(p_2, \begin{array}{c} \langle (u_1,q_1), 0.15,0.64,0.53\rangle, \langle (u_1,q_2), 0.48,0.62,0.88\rangle, \\ \langle (u_2,q_1), 0.74,0.34,0.25\rangle, \langle (u_2,q_2), 0.12,0.46,0.77\rangle \end{array}\right), \\ \left(p_3, \begin{array}{c} \langle (u_1,q_1), 0.65,0.84,0.14\rangle, \langle (u_1,q_2), 0.35,0.57,0.79\rangle, \\ \langle (u_2,q_1), 0.49,0.57,0.89\rangle, \langle (u_2,q_2), 0.91,0.26,0.72\rangle \end{array}\right), \\ \left(p_4, \begin{array}{c} \langle (u_1,q_1), 0.53,0.3,0.25\rangle, \langle (u_1,q_2), 0.77,0.87,0.93\rangle, \\ \langle (u_2,q_1), 0.22,0.32,0.19\rangle, \langle (u_2,q_2), 0.39,0.86,0.24\rangle \end{array}\right) \end{array} \right\},$$

In these cases, the effects and relationships between the parameters for television of different brands could be formulated. If $(\widehat{\Re}_Q^1, K \times L), (\widehat{\Re}_Q^2, L \times M)$ are Q-NS-sets from $(\hat{\Gamma}_Q, P)$ to $(\hat{\Lambda}_Q, P)$ and from $(\hat{\Lambda}_Q, P)$ to $(\hat{\Omega}_Q, P)$ correspondingly, where $K \times L \subseteq P \times P, L \times M \subseteq P \times P$ for $= \{p_1, p_3\}$, $L = \{p_4\}, M = \{p_2\}$, then Q-NS- relation can be given as:

$$(\widehat{\Re}_Q^1, K \times L) = \left\{ \begin{array}{l} \left((p_1,p_4), \begin{array}{c} \langle (u_1,q_1), 0.23,0.45,0.44\rangle, \langle (u_2,q_2), 0.44,0.55,0.75\rangle, \\ \langle (u_2,q_1), 0.25,0.73,0.92\rangle, \langle (u_2,q_2), 0.15,0.66,0.84\rangle \end{array}\right) \\ (p_3,p_4), \left(\begin{array}{c} \langle (u_1,q_1), 0.62,0.84,0.44\rangle, \langle (u_1,q_2), 0.35,0.57,0.79\rangle, \\ \langle (u_2,q_1), 0.33,0.73,0.92\rangle, \langle (u_2,q_2), 0.15,0.66,0.72\rangle \end{array}\right) \end{array} \right\}$$

$$\widehat{\Re}_Q^2, L \times M) = \left\{ \left((p_4,p_2), \begin{array}{c} \langle (u_1,q_1), 0.55,0.45,0.45\rangle, \langle (u_1,q_2), 0.49,0.65,0.22\rangle, \\ \langle (u_2,q_1),0.32,0.73,0.92\rangle, \langle (u_2,q_2),0.15,0.84,0.44\rangle \end{array}\right) \right\}$$

The Q-NS-set $(\widehat{\Re}_Q^1, K \times L)$ defines the effects of parameter in K can be "easy to use" where it evaluates the true, indeterminacy and false membership degree for the "fun to watch" or "modern" televisions from different brands as "easy to use". Likewise, the Q-NS-set $(\widehat{\Re}_Q^2, L \times M)$ express the effects of "easy to use" can be "expensive", where it evaluates the truth, indeterminacy and false membership degree for an "easy to use" television from different brands can be "expensive".

$$(\widehat{\Re}_Q^2 \circ \widehat{\Re}_Q^1, K \times M) = \left\{ \begin{array}{l} \left((p_1,p_2), \begin{array}{c} \langle (u_1,q_1),062,0.45,0.44\rangle, \langle (u_1 q_2),049,0.57,022\rangle, \\ \langle (u_2,q_1),0.32,0.73,0.92\rangle, \langle (u_2,q_2),0..15,0.66,0.44\rangle \end{array}\right) \\ (p_3,p_2), \left(\begin{array}{c} \langle (u_1,q_1), 0.62,0.84,0.44\rangle, \langle (u_1,q_2), 0.35,0.57,0.22\rangle, \\ \langle (u_2,q_1),0.33,0.73,0.92\rangle, \langle (u_2,q_2),0.15,0.66,0.44\rangle \end{array}\right) \end{array} \right\}$$

$T_{(\widehat{\Re}_Q^2 \circ \widehat{\Re}_Q^1)(a,c)}, I_{(\widehat{\Re}_Q^2 \circ \widehat{\Re}_Q^1)(a,c)}$ and $F_{(\widehat{\Re}_Q^2 \circ \widehat{\Re}_Q^1)(a,c)}$ correspondingly, the truth, indeterminacy and falsity degrees for "fun to watch" or "modern" televisions from different brands can be "expensive". The term $\langle (u_2,q_1),0.33,0.73,0.92\rangle$ for (p_3,p_2) implies that the "modern" of (u_2,q_1) has 0.33 truth membership function can be "expensive", 0.73 indeterminacy membership function can be "expensive", and 0.92 false membership function can be "expensive".

Consider$(\hat{\Gamma}_Q\alpha, \mathrm{P}), (\hat{\Lambda}_Q, \mathrm{P}), (\hat{\Omega}_Q, \mathrm{P}) \in 2^{\mathrm{NS_Q(U)}}$ and $\left(\widehat{\Re}_Q^1, \mathrm{K} \times \mathrm{L}\right), (\widehat{\Re}_Q^2, \mathrm{L} \times \mathrm{M})$ as Q-NS-sets from $(\hat{\Gamma}_Q, \mathrm{P})$ to $(\hat{\Lambda}_Q, \mathrm{P})$ and from $(\hat{\Lambda}, \mathrm{P})$ to (Ω_Q, P) correspondingly, where $\times$ LsubseteqP $\times$ P, $\mathrm{L} \times \mathrm{M} \subseteq \mathrm{P} \times \mathrm{P}$. Then

$(\widehat{\Re}_Q^2 \circ \widehat{\Re}_Q^1, K \times M)^{-1} = ((\widehat{\Re}_Q^1)^{-1} \circ (\widehat{\Re}_Q^2)^{-1}, M \times K).$

Since $(\widehat{\Re}_Q^1, K \times L), (\widehat{\Re}_Q^2, L \times M)$ are Q-NS-sets from $(\hat{\Gamma}_q, P)$ to $(\hat{\Lambda}_Q, P)$ and $(\hat{\Lambda}_Q, P)$ to $(\hat{\Omega}_Q, P)$ correspondingly, then $\left(\widehat{\Re}_Q^2 \circ \widehat{\Re}_Q^1, K \times M\right) \subseteq (\hat{\Gamma}_Q, P) \wedge\times (\hat{\Omega}_Q, P)$. Therefore, for $(a,c) \in K \times M, (u,q) \in U \times Q$,

DOI: https://doi.org/10.54216/IJNS.250117
Received: April 27, 2024 Revised: June 05, 2024 Accepted: June 29, 2024

$$T_{(\widehat{\Re}_Q^2 \circ \widehat{\Re}_Q^1)^{-1}(a,c)}(u,q) = T_{(\widehat{\Re}_Q^2 \circ \widehat{\Re}_Q^1)(a,c)}(u,q)$$

$$= \max\left\{T_{\widehat{\Re}_Q^1(a,b)}(u), T_{\widehat{\Re}_Q^2(b,c)}(u)\right\}$$

$$= \max\{T_{\widehat{\Re}_Q^2(b,c)}(u,q), T_{\widehat{\Re}_Q^1(a,b)}(u,q)\}$$

$$= \max\left\{\min\left\{T_{\widehat{\Lambda}_Q(b)}(u,q), T_{\widehat{\Omega}_Q(c)}(u,q)\right\}, \min\left\{T_{\widehat{\Gamma}_Q(a)}(u,q), T_{\widehat{\Lambda}_Q(b)}(u,q)\right\}\right\}$$

$$= \max\left\{\min\left\{T_{\widehat{\Omega}_Q(c)}(u,q), T_{\widehat{\Lambda}_Q(b)}(u,q)\right\}, \min\left\{T_{\widehat{\Lambda}_Q(b)}(u,q), T_{\widehat{\Gamma}_Q(a)}(u,q)\right\}\right\}$$

$$= \max\{\tau_{(\widehat{\Re}_Q^2)^{-1}(c,b)(\widehat{\Re}_Q^1)^{-1}(b,a)}(u,q), T(u,q)\}$$

$$= T((\widehat{\Re})^{-1} \circ (\widehat{\Re})^{-1})(c,a)(u,q)$$

Comparable outcomes can be revealed for $I(\widehat{\Re}_Q^2 \circ \widehat{\Re}_Q^1)^{-1}(c,a)(u,q)$ and $(\widehat{\Re}_Q^2 \circ \widehat{\Re}_Q^1)^{-1}(c,a)(u,q)$.

4. Result Analysis

The performance analysis of the QNSRDL-PLDR technique is studied using Plant village dataset, from Kaggle repository [21]. The dataset involves 2475 samples with two classes are represented in Table 1.

Table 1: Details of dataset

Class	No. of Samples
Bacterial Spot	997
Healthy	1478
Total Samples	2475

In Table 2 and Fig. 3, brief detection results of the QNSRDL-PLDR approach on 80%TRP and 20% TSP are described. The experimental values pointed out that the QNSRDL-PLDR technique properly recognized the samples. With 80%TRP, the QNSRDL-PLDR technique offered average $accu_y$, $prec_n$, $reca_l$, F_{score}, and AUC_{score} of 94.95%, 96.53%, 94.95%, 95.59%, and 94.95%, correspondingly. Meanwhile, with 20%TSP, the QNSRDL-PLDR method provided average $accu_y$, $prec_n$, $reca_l$, F_{score}, and AUC_{score} of 94.60%, 96.61%, 94.60%, 95.43%, and 94.60%, correspondingly.

Table 2: Detection outcome of QNSRDL-PLDR technique on 80%TRP and 20% TSP

Class	$Accu_y$	$Prec_n$	$Reca_l$	F_{Score}	AUC_{Score}
TRP (80%)					
Bacterial Spot	90.32	99.32	90.32	94.61	94.95
Healthy	99.57	93.74	99.57	96.57	94.95
Average	94.95	96.53	94.95	95.59	94.95
TSP (20%)					
Bacterial Spot	89.53	99.42	89.53	94.21	94.60
Healthy	99.67	93.81	99.67	96.65	94.60
Average	94.60	96.61	94.60	95.43	94.60

DOI: https://doi.org/10.54216/IJNS.250117
Received: April 27, 2024 Revised: June 05, 2024 Accepted: June 29, 2024

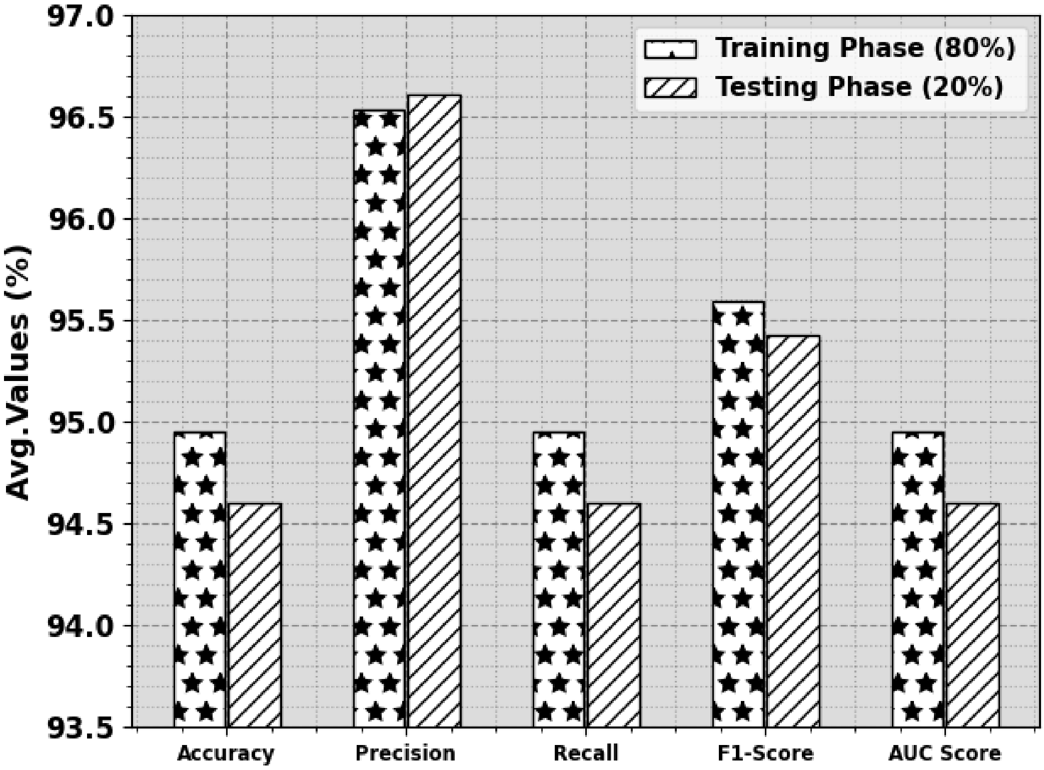

Figure 3: Average of QNSRDL-PLDR technique on 80%TRP and 20% TSP

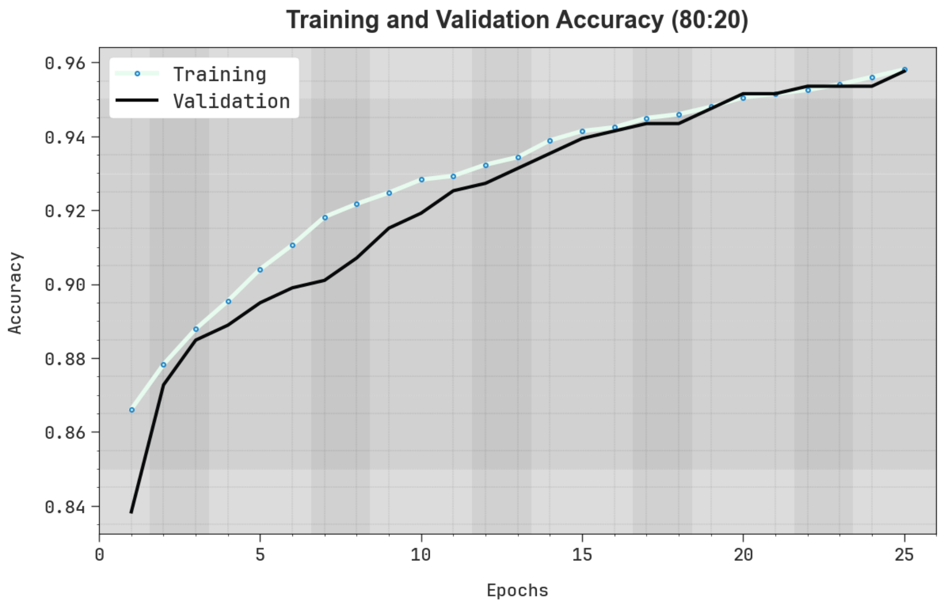

Figure 4: $Accu_y$ curve of QNSRDL-PLDR technique on 80%TRP and 20%TSP

In Fig. 4, the training and validation accuracy outcomes of the QNSRDL-PLDR method on 80%TRP and 20%TSP are illustrated. The figure emphasized that the training and validation accuracy values show a growing tendency which notified the capability of the QNSRDL-PLDR approach with greater efficiency over various iterations.

In Fig. 5, the training and validation loss graph of the QNSRDL-PLDR method on 80%TRP and 20%TSP is exhibited. It is indicated that the training and validation accuracy values illustrate a declining tendency, notifying the capability of the QNSRDL-PLDR method to balance a tradeoff between data fitting and generalization.

DOI: https://doi.org/10.54216/IJNS.250117
Received: April 27, 2024 Revised: June 05, 2024 Accepted: June 29, 2024

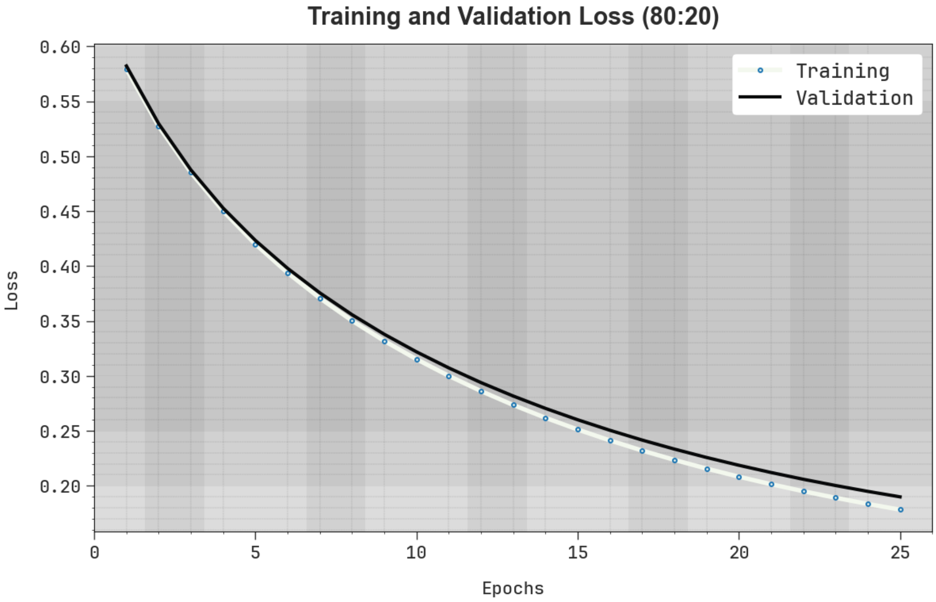

Figure 5: Loss curve of QNSRDL-PLDR approach on 80%TRP and 20%TSP

In Table 3 and Fig. 5, brief detection results of the QNSRDL-PLDR approach on 70%TRP and 30% TSP are depicted. The outcomes indicated that the QNSRDL-PLDR approach accurately detected the samples. With 70%TRP, the QNSRDL-PLDR method provided average $accu_y$, $prec_n$, $reca_l$, F_{score}, and AUC_{score} of 93.87%, 94.01%, 93.87%, 93.94%, and 93.87%, correspondingly. Meanwhile, With 30%TSP, the QNSRDL-PLDR method provided average $accu_y$, $prec_n$, $reca_l$, F_{score}, and AUC_{score} of 93.83%, 94.09%, 93.83%, 93.95%, and 93.83%, correspondingly.

Table 3: Detection outcome of QNSRDL-PLDR technique on 70%TRP and 30% TSP

Class	$Accu_y$	$Prec_n$	$Reca_l$	F_{Score}	AUC_{Score}
TRP (70%)					
Bacterial Spot	92.29	93.22	92.29	92.75	93.87
Healthy	95.45	94.80	95.45	95.12	93.87
Average	93.87	94.01	93.87	93.94	93.87
TSP (30%)					
Bacterial Spot	91.92	93.49	91.92	92.70	93.83
Healthy	95.74	94.68	95.74	95.21	93.83
Average	93.83	94.09	93.83	93.95	93.83

In Table 4, a widespread comparison study is made to guarantee the enhanced performance of the QNSRDL-PLDR method [16]. The experimental values stated that the ResNet-50, DenseNet-121, and ShuffleNetV2 models have gained worse performance over other models. Moreover, the MobileNetV1, ResNeXt-50, and EfficientNet-B0 models have obtained closer performance compared to recent models. Nevertheless, the QNSRDL-PLDR technique demonstrates better performance with maximum $prec_n$, $F1_{score}$, $reca_l$, and $accu_y$ of 96.53%, 95.59%, 94.95%, and 94.95%, correspondingly. Therefore, the QNSRDL-PLDR technique can be applied for enhanced pepper leaf disease detection process.

Table 4: Comparative analysis of QNSRDL-PLDR technique with existing approaches

Methods	$Prec_n$	$F1_{Score}$	$Reca_l$	$Accu_y$
ResNet-50	93.31	93.86	90.57	90.29
DenseNet-121	94.65	92.83	92.48	92.06
MobileNetV1	95.62	93.34	91.98	92.03
ShuffleNetV2	94.85	93.42	92.95	92.48

DOI: https://doi.org/10.54216/IJNS.250117
Received: April 27, 2024 Revised: June 05, 2024 Accepted: June 29, 2024

ResNeXt-50	96.03	90.14	93.36	93.22
EfficientNet-B0	96.06	92.54	93.05	93.82
QNSRDL-PLDR	96.53	95.59	94.95	94.95

5. Conclusion

In this study, we have developed a new QNSRDL-PLDR method for sustainable agriculture in KSA. The main purposes of the QNSRDL-PLDR technique contain three distinct processes involved feature extraction, parameter optimizer, and classification process. Initially, the proposed QNSRDL-PLDR method leverages DenseNet for feature extraction, the model uses the Adam optimizer for effective parameter optimization. Unique to this framework is the combination of a Q-neutrosophic soft relation classifier, allowing nuanced classification considering truth, indeterminacy, and falsity degrees in disease presence assessment. A comprehensive set of simulations is conducted to demonstrate the better performance of the QNSRDL-PLDR technique. This technique aims to improve reliability and accuracy in detecting Pepper Leaf Diseases, critical for crop management and sustainable agricultural practices.

Funding: “The authors extend their appreciation to Prince Sattam bin Abdulaziz University for funding this research work through the project number (PSAU/2024/01/29590)”

Conflicts of Interest: “The authors declare no conflict of interest.”

References

[1] Noaman, I.A.R., Hasan, A.H. and Ahmed, S.M., 2024. Optimizing Weibull Distribution Parameters for Improved Earthquake Modeling in Japan: A Comparative Approach. International Journal of Neutrosophic Science, 24(1), pp.65-5.

[2] Doaa Nihad Tomma, L. A. A. Al-Swidi. "Necessary and Sufficient Conditions for a Stability of the Concepts of Stable Interior and Stable Exterior via Neutrosophic Crisp Sets." International Journal of Neutrosophic Science, Vol. 24, No. 1, 2024 ,PP. 87-93

[3] Mathews, P., Sebastian, L. and Thankachan, B., 2024. Neutrosophic Fuzzy Score Matrices: A Robust Framework for Advancing Medical Diagnostics. International Journal of Neutrosophic Science, 23(3), pp.08-8.

[4] R. Saarumathi, W. Ritha. (2024). A Legitimate Productive Repertoire Replica Betwixt Envirotech Outlay Towards Fragile Commodities Using Trapezoidal Neutrosophic Fuzzy Number. International Journal of Neutrosophic Science, 24 (1), 104-118.

[5] Eunice, J., Popescu, D.E., Chowdary, M.K. and Hemanth, J., 2022. Deep learning-based leaf disease detection in crops using images for agricultural applications. Agronomy, 12(10), p.2395.

[6] Jha, P., Dembla, D. and Dubey, W., 2024. Implementation of Transfer Learning Based Ensemble Model using Image Processing for Detection of Potato and Bell Pepper Leaf Diseases. International Journal of Intelligent Systems and Applications in Engineering, 12(8s), pp.69-80.

[7] Kapoor, K., Singh, S., Singh, N.P. and Priyanka, 2023, January. Bell-Pepper Leaf Bacterial Spot Detection Using AlexNet and VGG-16. In International Conference on Smart Trends for Information Technology and Computer Communications (pp. 507-519). Singapore: Springer Nature Singapore.

[8] Kaur, A., Kukreja, V., Gopal, L., Verma, G. and Sharma, R., 2024, January. Next-Gen Hybrid Deep Learning for Accurate Pepper Leaf Mosaic Virus Classification. In 2024 International Conference on Intelligent and Innovative Technologies in Computing, Electrical and Electronics (IITCEE) (pp. 1-4). IEEE.

[9] Ullah, N., Khan, J.A., Almakdi, S., Alshehri, M.S., Al Qathrady, M., Aldakheel, E.A. and Khafaga, D.S., 2023. A Lightweight Deep Learning-Based Model for Tomato Leaf Disease Classification. Computers, Materials & Continua, 77(3).

[10] Mahesh, T.Y. and Mathew, M.P., 2023. Detection of bacterial spot disease in bell pepper plant using YOLOv3. IETE Journal of research, pp.1-8.

[11] Priya, D.T. and Vijayarani, A., 2024. Plant Disease Detection and Classification Using a Deep Learning Approach for Image-Based Data. In Intelligent Systems and Sustainable Computational Models (pp. 352-368). Auerbach Publications.

[12] Perveen, K., Debnath, S., Pandey, B., Chand, S.P., Bukhari, N.A., Bhowmick, P., Alshaikh, N.A., Arzoo, S. and Batool, S., 2023. Deep learning-based multiscale CNN-based U network model for leaf disease diagnosis and segmentation of lesions in tomato. Physiological and Molecular Plant Pathology, 128, p.102148.

DOI: https://doi.org/10.54216/IJNS.250117
Received: April 27, 2024 Revised: June 05, 2024 Accepted: June 29, 2024

[13] Chen, R., Qi, H., Liang, Y. and Yang, M., 2022. Identification of plant leaf diseases by deep learning based on channel attention and channel pruning. Frontiers in plant science, 13, p.1023515.

[14] Sarawagi, K., Dhiman, H., Pagrotra, A. and Talwandi, N.S., 2024. Deep Learning for Early Disease Detection: A CNN Approach to Classify Potato, Tomato, and Pepper Leaf Diseases.

[15] Abisha, S., Mutawa, A.M., Murugappan, M. and Krishnan, S., 2023. Brinjal leaf diseases detection based on discrete Shearlet transform and Deep Convolutional Neural Network. Plos one, 18(4), p.e0284021.

[16] Wan, L., Zhu, W., Dai, Y., Zhou, G., Chen, G., Jiang, Y., Zhu, M.E. and He, M., 2024. Identification of Pepper Leaf Diseases Based on TPSAO-AMWNet. Plants, 13(11), p.1581.

[17] Rababa, L., Ali, N., Alessa, R. and Alzu'bi, A., 2023, November. Pepper Leaf Diagnosis Using Deep-Net with Low-Dimensional Image Classification. In 2023 14th International Conference on Information and Communication Systems (ICICS) (pp. 1-5). IEEE.

[18] Nalluri, S. and Sasikala, R., 2024. A deep neural architecture for SOTA pneumonia detection from chest X-rays. International Journal of System Assurance Engineering and Management, 15(1), pp.489-502.

[19] Liao, Y., Lu, S. and Yin, G., 2024. Short-Term and Imminent Rainfall Prediction Model Based on ConvLSTM and SmaAT-UNet. Sensors, 24(11), p.3576.

[20] Dalkılıç, O. and Demirtaş, N., 2023. A novel perspective for Q-neutrosophic soft relations and their application in decision making. Artificial Intelligence Review, 56(2), pp.1493-1513.

[21] https://www.kaggle.com/datasets/adilmubashirchaudhry/plant-village-dataset

DOI: https://doi.org/10.54216/IJNS.250117
Received: April 27, 2024 Revised: June 05, 2024 Accepted: June 29, 2024